Plasticity of Acetylcholine Receptor Gating Motions via Rate-Energy Relationships

Ananya Mitra, Richard Tascione, Anthony Auerbach, and Stuart Licht
Center for Single Molecule Biophysics and the Department of Physiology and Biophysics, The State University of New York, Buffalo, New York

ABSTRACT Like other protein conformational changes, ion channel gating requires the protein to achieve a high-energy transition-state structure. It is not known whether ion channel gating takes place on a broad energy landscape on which many alternative transition state structures are accessible, or on a narrow energy landscape where only a few transition-state structures are possible. To address this question, we measured how rate-equilibrium free energy relationships (REFERs) for di-liganded and unliganded acetylcholine receptor gating vary as a function of the gating equilibrium constant. A large slope for the REFER plot indicates an openlike transition state, whereas a small slope indicates a closedlike transition state. Due to this relationship between REFERs and transition-state structure, the sensitivity of the REFER slope to mutation-induced energetic perturbations allows estimation of the breadth of the energy landscape underlying gating. The relatively large sensitivity of di-liganded REFER slopes to energetic perturbations suggests that the motions underlying di-liganded gating take place on a broad, shallow energy landscape where many alternative transition-state structures are accessible.

INTRODUCTION

Ion channels close and open (gate) by means of complex protein conformational changes. Recent studies (1–5) have provided insight into the structures of closed and open channel conformations. However, the details of the protein motions that make up these global changes in structure are just beginning to be investigated. Recent work has shown that for the acetylcholine receptor channel (AChR), the opening conformational change initiates at the transmitter binding site and propagates through the channel structure asynchronously, approximately as a coarse-grained wave (6). In this picture, the transition state of AChR gating is not reducible to a single conformation that is globally intermediate between the stable open and closed conformations. Although gating proceeds through a single pathway, the transition region in this pathway consists of an ensemble of conformations, within which some parts of the protein resemble the open conformation whereas others resemble the closed conformation.

Given the complexity of the transition-state ensemble, there may not be many alternative transition-state structures that can support rapid gating. Alternatively, if large segments of the protein can move as relatively rigid and independent units (7), it might be possible for them to adopt many transition-state structures that are easily accessible from the ground state. A channel with the latter properties might have the advantage of being robust to mutations, since it could adopt a different transition-state structure in response to the energetic perturbations caused by mutations.

The plasticity of the transition state to energetic perturbation serves as a measure of the accessibility of alternative transition states. If many alternative transition states are relatively accessible, small energetic perturbations will be able to introduce appreciable shifts in the transition-state structure. Although the transition-state conformation is not directly measurable, its properties can be inferred from the analysis of rate-equilibrium free energy relationships (REFERs) (8,9). When this relationship is linear, its slope (ϕ) gives the position of the transition state along the reaction coordinate.

REFERs can also be used to investigate the plasticity of transition-state structure. Curvature in REFERs implies plasticity of the transition state (i.e., a change in its position along the reaction surface) and provides information about its structure. The effects of energetic perturbations on transition states have been studied extensively in physical organic chemistry (8,10,11), protein folding (12,13), enzymatic catalysis (14,15), and other protein conformational changes (16,17).

Previous work has shown that relatively small energetic perturbations caused by a site-directed mutation at a single position generally give rise to linear REFERs (6,18,19), suggesting that such perturbations do not make detectable changes in the position of the transition state. However, in covalent reactions (8) and protein folding reactions (20), substitutions at remote positions can have large effects (known as Hammond effects) on ϕ-values. For the AChR, probing the transition-state structure for unliganded gating, which is highly thermodynamically unfavorable compared to di-liganded gating, revealed that the transition state for unliganded gating is globally similar to the closed state (21). The experiments of Grosman (21) suggest that there is at

Submitted June 14, 2005, and accepted for publication July 26, 2005.

This article is dedicated to the memory of Rick Tascione, who passed away while it was being prepared.

Address reprint requests to S. Licht, Tel.: 617-452-3525; E-mail: lichts@mit.edu.

0006-3495/05/11/3071/08 $2.00

doi: 10.1529/biophysj.105.068783

least one accessible transition state structure that differs significantly from the transition state for di-liganded opening.

Here, we quantify the plasticity of the transition state for di-liganded opening itself by measuring REFERs in AChRs having different mutational backgrounds. We use the measured plasticity of the transition state to estimate the curvature of the reaction surface and its approximate timescale, and compare these values to the values derived from an independent estimate of the timescale of AChR gating dynamics (22).

METHODS

Channel expression

All mutations of the mouse muscle AChR subunits were engineered using the QuikChange Site-Directed Mutagenesis Kit (Stratagene, La Jolla, CA). The constructs were confirmed by dideoxy sequencing. Wild-type and mutant ACh receptors were transiently transfected via calcium phosphate precipitation in HEK293 cells. Thirty-five millimeter cell culture dishes were plated 24–48 h before transfection to be 50% confluent at the time of the transfection. Fourteen micrograms of mouse muscle cDNA (5.6 μg α, 2.8 μg each β-, δ-, and ε-subunits), 38 μl of $CaCl_2$, and ~300 μl water was layered on 350 μl buffer (NaCl, HEPES, and Na_2HPO_4). One-hundred-seventy-five microliters of the final mixture were added to each of four culture dishes. The medium was changed after 20–24 h and the cells patched 12–48 h later.

Electrophysiology

Single-channel recordings were made using the cell-attached patch clamp technique. Dulbecco's PBS was used as the bath solution and either PBS or K^+-Ringers (142 mM KCl, 5.4 mM NaCl, 1.8 mM $CaCl_2$, 1.7 mM $MgCl_2$, and 10 mM HEPES pH 7.4) was used as the pipette solution (with or without agonist). Before recording the culture medium was removed, and cells washed once with room temperature PBS. The patch membrane potential was −70 to −100 mV. The ambient temperature was 22–24°C for all recordings. The data were filtered at 10–30 kHz, sampled at 40–100 kHz and saved directly to hard disk.

Kinetic analysis

Data acquisition, rate constant estimation, and kinetic simulations were carried out using QuB software (*www.qub.buffalo.edu*). In 20 mM choline, openings occurred in clusters, with long gaps between clusters reflecting sojourns in desensitized states. Clusters of openings were selected either by eye or by invoking a critical closed-interval duration (t_{crit}) of 20–50 ms. Selected currents were idealized into noise-free intervals using a $C \rightleftarrows O$ model with a starting rate constant of 10 s^{-1} and segmental *k*-means algorithm (23). The apparent opening and closing rate constants were estimated from these idealized sequences using maximum-likelihood algorithm (24,25) after imposing a dead-time of 33–75 μs. We used a two-state, $C \rightleftarrows O$ model with a starting rate constant 100 s^{-1} for both. In some cases, an additional, uncoupled closed state to incorporate sojourns in a short-lived desensitized state was used (26). The apparent gating equilibrium constant (Θ) was computed as the ratio of the opening rate constant (β) and the closing rate constant (α).

We measured the di-liganded channel closing rate constant (α) for series of mutations at δS268 (the 12′ position of the M2 transmembrane segment) in the presence of different background, loss-of-function mutations. Specifically, the background mutants were αT422A (in the transmembrane, M4 segment), εP121L (in the extracellular domain), and the double-mutant construct αT422A+εP121L. Di-liganded channel openings were elicited by using 200 μM or 500 μM choline and α was determined from the inverse of the open channel duration (27,28).

The opening rate constants (β) were too slow to give rise to clusters of openings and closings even in saturating (20 mM) choline and could not be measured directly. We therefore calculated opening rate constants from the closing rate constant and an estimate of the gating equilibrium constant ($\Theta = \beta/\alpha$). To estimate Θ, we assumed that effects of mutations and agonists were energetically independent. Previous work using several mutant AChRs has shown that mutations in the AChR have the same energetic effects on unliganded and di-liganded receptors (26,28), and that mutations in different subunits of the channel have energetically independent effects on gating (28). It is thus reasonable to believe that energetic perturbations due to structural perturbations at distinct regions of the channel will typically be energetically independent. With this assumption, we were able to use the previously measured effects on Θ of the individual background mutations αT422A (~50-fold decrease (29)) and εP121L, (500-fold decrease (30)) to estimate the Θ for constructs containing a mutation at δS268 and one or both background positions. These calculated Θ-values and the experimentally-determined α-values were used to obtain estimates of β for each construct.

REFER analysis

We determined the position of the transition state along the reaction coordinate using rate-equilibrium free energy relationship (REFER) analysis (8). The rate constant of the channel-opening reaction is plotted as a function of the gating equilibrium constant, on a log-log plot. The slope of this plot, called ϕ, is related to the position of the transition state. High values of ϕ (i.e., close to *1*) are consistent with an openlike transition state, whereas low values (i.e., close to *0*) are consistent with a closedlike transition state. The magnitude of the shift in ϕ after background perturbations, $\delta\phi/\delta\Delta G$, is an index of the plasticity of the transition state (8,9).

Since channel gating is a process with an activation barrier (i.e., with Markovian kinetics), it is reasonable to describe the rate constant for gating using the expression

$$k = A^* \times \exp\left(\frac{-\Delta G^{\ddagger}}{RT}\right), \quad (1)$$

where $\Delta G^{\ddagger}$ is the activation energy and A^* is a pre-exponential factor that depends on the timescale of the dynamics underlying the reaction. The barrier height when the open state and closed state have the same free energy

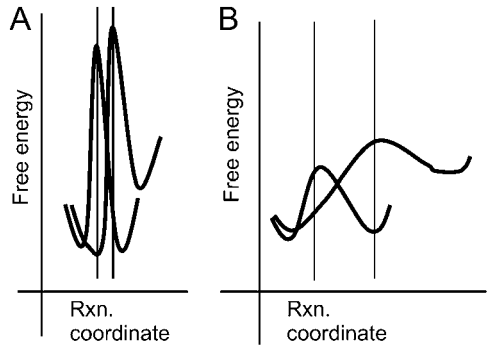

FIGURE 1 Illustration of a Hammond effect and its relationship to the intrinsic barrier. (*A*) For steep, narrow wells, the intrinsic barrier is high, and a perturbation does not have a large effect on the position of the transition state (*narrow lines*). (*B*) For broad, shallow wells, the intrinsic barrier is low, and the magnitude of the Hammond effect is large.

(i.e., the gating equilibrium constant is 1) is called the intrinsic barrier to reaction (γ).

The method used here to estimate $\Delta G^{\ddagger}$ depends on the relationship between the size of the activation barrier and the effect of energetic perturbations on transition-state structure. A simple picture of the reaction, based on Marcus reaction rate theory (31), uses a single reaction coordinate (i.e., some structural parameter that differs between the open and closed states) to describe the progress of the reaction. Fig. 1 shows a cartoon of a free energy versus reaction coordinate diagram for the gating reaction. The stable open and closed states are modeled as the local minima in parabolic wells: that is, their structures fluctuate about an average structure. The transition state is the intersection between the parabolas. For a protein conformational change, the shape of the potentials is not required to be parabolic; the quantitative treatment described in the Appendix uses a parabolic potential for the sake of simplicity.

In this simple model, the width of the wells determines the effect of perturbations on the position of the transition state along the reaction coordinate (i.e., the transition-state structure). The point of intersection between the closed state and open state potentials determines the position of the transition state. Thus, the geometry of the wells influences the effect of energetic perturbations on the position of the transition state (Fig. 1). When the wells are narrow (Fig. 1 *A*), the effect of perturbations is small, whereas when the wells are broad, the effect is larger (Fig. 1 *B*). The shape of the wells also determines the barrier height when the open state and closed state have the same free energy (i.e., the gating equilibrium constant is *1*): this barrier height is called the intrinsic barrier to reaction. The intrinsic barrier is high when the wells are narrow and lower when the wells are broad. Thus, the intrinsic barrier is linked to the effect of perturbations on transition-state structure through their mutual dependence on the geometry of the reaction surface.

RESULTS

Di-liganded gating ϕ-value for position δ269 in the wild-type background

We measured the single-channel gating kinetics for a series of mutations (G, C, T, I, and N) at δS268, a residue located at the 12′ position of the δ-subunit M2 membrane-spanning segment (32). Fig. 2 shows single-channel currents obtained from a series of six side-chain substitutions at δ268 position using 20 mM choline as agonist. All the mutants increased the gating equilibrium constant (Θ), mainly by decreasing the closing rate constant. The δ268N mutation showed the greatest increase in Θ. The REFER for position δ268 was approximately linear with a slope (Φ) of 0.14 ± 0.02 (mean ± SD; Fig. 3). This ϕ-value is less than reported previously (0.28 ± 0.02; (6,33). The reason for this difference is unclear, but may relate to the difference in the ionic composition of the pipette solution (PBS versus K^+-Ringers). For the purposes of this study, however, the relevant parameter is the change of ϕ-value within the series of mutant backgrounds, and experimental conditions that may affect the ϕ-value are uniform within the series of experiments presented here. The small ϕ-value for δS268 suggests that in the wild-type background this residue moves relatively late in the di-liganded gating reaction.

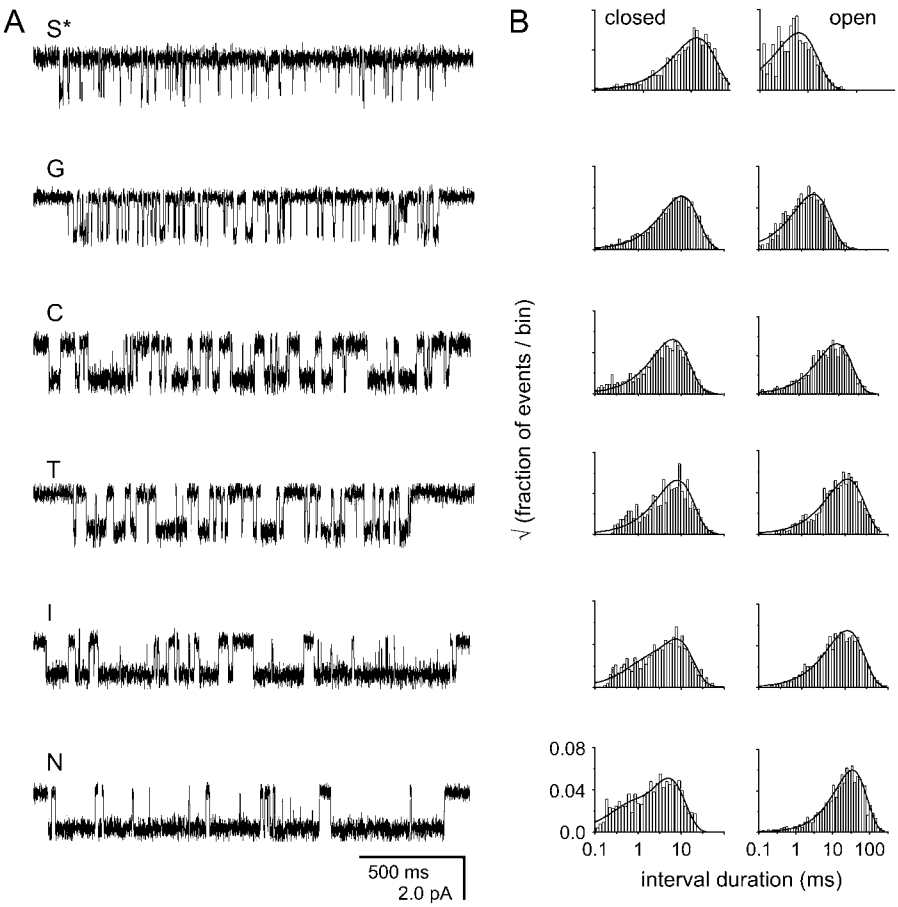

FIGURE 2 (*A*) Representative single-channel currents obtained from a series of six side-chain substitutions at position δ268. Currents were elicited with saturating choline (20 mM) in a wild-type background. Openings are downwards. Capital letters indicate the identity of the substitution at δS268. (*B*) Open and closed time histograms and fitted probability density function of the δ268I mutant series.

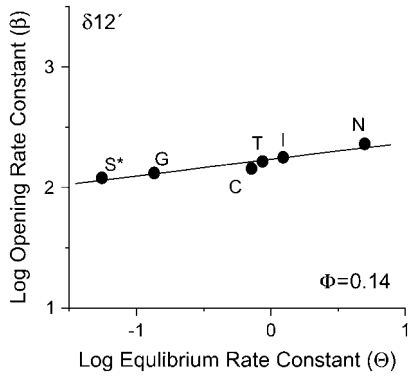

FIGURE 3 REFER plot for the δ268 mutant series. Each point represents the average of greater than three patches.

Di-liganded gating ϕ-values for position δ269 with background mutations

To study the effect of energetic perturbations on the transition state as probed by δ268 mutant series, we studied the single channel behavior of the δ268 mutants in the context of various loss-of-function background mutations (Table 1). These background mutations are single-point mutations in different subunits, and are located far from the δ268 position in the channel structure (34). The αT422A mutation is located at the 14′ position in the αM4 transmembrane segment and results in a 35-fold reduction in Θ ($\phi = 0.54$; (29)). In the presence of this background mutation, the REFER plot of the δS268 constructs had an approximately linear slope, with $\phi = 0.31 \pm 0.04$ (Fig. 4). A comparison of the REFER plot of the δS268 constructs in the wild-type background and those of the δS268 constructs in the αT422A background mutation gives a $\delta\phi/\delta\Delta G_0$ of $0.048 \pm 0.01\ k_BT^{-1}$ (although this value must be interpreted with caution, because it comes from only two REFER plots).

The gating behavior of the δS268 mutant series in the presence of the background mutation εP121L, which is in the extracellular domain of the ε-subunit and which by itself causes a ~500-fold reduction in Θ (30), was also determined (Fig. 4). In this background, the observed channel closing rate constants were similar for all δ269 mutants, ~12,000 s^{-1}. By recasting the estimated gating rate constants of the δS269 mutant series as a REFER, we obtain $\phi = 0.78 \pm 0.03$. For the εP121L background mutation, $\delta\phi/\delta\Delta G_0$ cal-

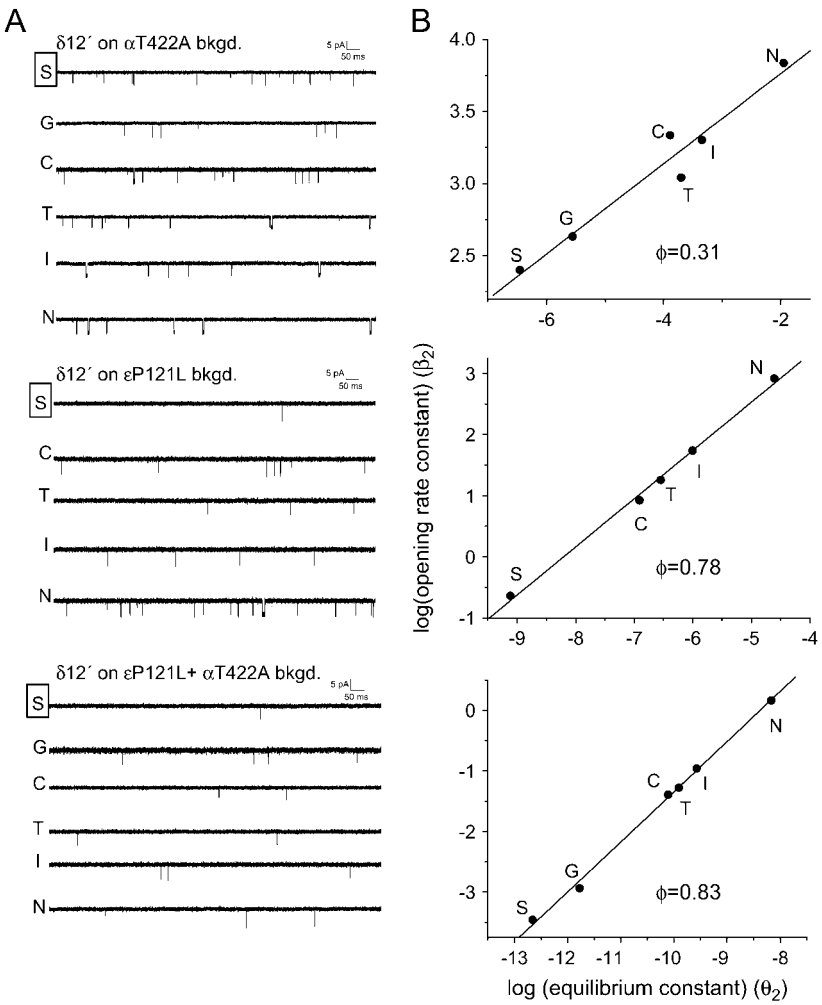

FIGURE 4 (*A*) Representative single-channel currents obtained from a series of different side-chain substitutions at position δS268 in the presence of αT422A (35-fold loss-of-function), εP121L (~500-fold loss-of-function), and εP121L+αT422A (~25,000-fold loss-of-function) backgrounds, respectively. Currents were elicited with a low concentration of choline (200 μM for αT422A and 500 μM for εP121L and εP121L+αT422A backgrounds). Openings are downwards. (*B*) REFER plots for the δS268 mutant series on different backgrounds. (*Top*) αT422A, (*middle*) εP121L, and (*bottom*) εP121L+αT422A.

TABLE 1 Gating rate and equilibrium constants

Construct	Opening rate constant (s^{-1})	Closing rate constant (s^{-1})	Gating equilibrium constant (Θ)
δ268S	120	2170	0.055
δ268G	131	967	0.136
δ268C	143	200	0.715
δ268T	164	190	0.863
δ268I	177	143	1.23
δ268N	228	45.8	4.98
δ268S + αT422	11.0	7020	1.57 E^{-3}
δ268G + αT422	13.9	3600	3.86 E^{-3}
δ268C + αT422	28.0	1373	0.020
δ268T + αT422	20.9	846	0.025
δ268I + αT422	27.2	770	0.035
δ268N + αT422	46.2	325	0.142
δ268S + εP121L	0.75	4780	1.57 E^{-4}
δ268C + εP121L	3.60	2530	1.42 E^{-3}
δ268T + εP121L	5.00	2450	2.04 E^{-3}
δ268I + εP121L	8.10	2300	3.52 E^{-3}
δ268N + εP121L	26.4	1850	0.014
δ268S + αT422+ εP121L	0.03	9890	3.03 E^{-6}
δ268G + αT422+ εP121L	0.05	6880	7.26 E^{-6}
δ268C + αT422+ εP121L	0.25	6090	4.11 E^{-5}
δ268T + αT422+ εP121L	0.28	5570	5.03 E^{-5}
δ268I + αT422+ εP121L	0.38	5480	6.93 E^{-5}
δ268N + αT422+ εP121L	1.18	4140	2.85 E^{-4}

culated from two REFER plots was $0.103 \pm 0.006\ k_BT^{-1}$, which is greater than twofold larger than the corresponding value for the αT422A background.

Finally, we studied the gating kinetics of the δ268 mutant series in a background construct having both the αT422A and the εP121L mutations (Fig. 4). Assuming independence, we expect this combination to cause a 17,500-fold reduction in Θ. As was the case for the εP121L background alone, observed channel-closing rate constants were similar for all δ269 mutants, ~12,000 s^{-1}. The overall level of channel activity in the εP121L+αT422A patches was much smaller than with either background mutant alone, suggesting that Θ was indeed smaller in the double-mutant construct than the single-mutant constructs. A REFER analysis for the double-mutant background series showed $\phi = 0.83 \pm 0.02$, which is not significantly different from the value obtained with the εP121L background.

The effects of the background energetic perturbations on the φ-values of δ269 for di-liganded gating are illustrated in Fig. 5. Background mutations that make opening less thermodynamically favorable (i.e., decrease the gating equilibrium constant) also increase the φ-value. This observation is consistent with the transition-state structure (probed at position δS268) becoming more openlike as the opening reaction becomes more thermodynamically unfavorable; i.e., a Hammond effect (8). The slope of the plot in Fig. 5 *B*, which includes all of the background mutations used, is $\delta\phi/\delta\Delta G = -0.075 \pm 0.02\ k_BT^{-1}$.

DISCUSSION

Effect of background mutations on the transition state for gating

For di-liganded gating, we observe that large energetic perturbations due to background mutations exert a significant effect on the φ-values measured for position δ268. This result is qualitatively consistent with energetic/structural perturbations of the AChR ground states (open and closed) having a significant effect on the energetics/structure of the transition state, as has previously been observed through comparison of di-liganded and unliganded AChR gating (21). The magnitude of the observed shift in φ for all of the backgrounds, $-0.075\ k_BT^{-1}$, is large compared to analogous parameters measured for reactions of small molecules (8,10,11), but comparable to those measured for protein folding reactions (20,35,36). This suggests that the transition-state structure for di-liganded AChR gating is more sensitive to changes in free energy than typical transition states for covalent reactions, but comparable to those for protein folding.

Although changes in conformation within folded states are likely to be mechanistically different from folding transitions, both kinds of reactions are similar in that they involve large-scale polypeptide motions. Both folding reactions and

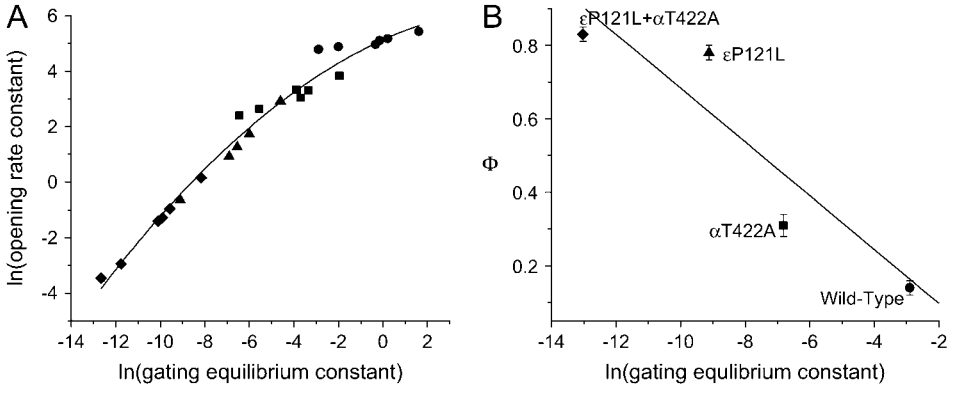

FIGURE 5 Change in REFER φ with the di-liganded gating equilibrium constant for the δS268 mutant series. (*A*) REFER plot of δ268 (six side chains; each point represents at least three patches) for all four backgrounds: wild-type (*circles*), αT422A (*squares*), εP121L (*triangles*), and εP121L+αT422A (*diamonds*). As the gating equilibrium constant is reduced there is a corresponding increase in φ (slope), from 0.14 (for wild-type background) to 0.83 (for εP121L+αT422). This curvature is consistent with a Hammond effect. (*B*) The φ-values obtained from linear fits for each background. The φ changes by $-0.075 \pm 0.02\ k_BT^{-1}$.

allosteric conformational changes may thus take place on potential energy surfaces that are broad and malleable compared to those observed for covalent reactions. Miyashita et al. have recently argued that allosteric conformational changes in proteins can be directly analogous to protein unfolding: they model the allosteric conformational change as a partial unfolding, or cracking, process (37,38).

Quantitative analysis of the effect of background mutations on the gating transition state

Chakrapani and Auerbach (22) estimated the intrinsic barrier and timescale of di-liganded (by ACh) AChR gating from the asymptote of the burst duration in mutants having a large opening rate-constant. These estimates were $\gamma = 6.1\ k_BT$ and $A = 8.6 \times 10^5\ s^{-1}$ (22). In principle, it should be possible to link the curvature of REFER plots to the size of the intrinsic barrier and the timescale of the reaction (31). Magnitudes of intrinsic barriers (the barrier height when the equilibrium constant is *1*) have been estimated in this way for covalent reactions of small molecules. Analyzing rate-equilibrium behavior of proton exchange between substituted benzoic acids (11), Grunwald calculated intrinsic barriers to reaction of ~17 kT (10 kcal/mol). These reactions have rate constants $\sim 10^5\ s^{-1}$, so, using Eq. 1, we can estimate a pre-exponential factor of $\sim 10^{12}\ s^{-1}$ for these reactions. Although the magnitude of the pre-exponential factor is not strictly identical to the speed-limit for a reaction (39), this value is consistent with the underlying dynamics of proton transfer occurring on the picosecond timescale, the timescale of molecular vibrations (defined by k_BT/h). Spectroscopic experiments on covalent reactions have provided experimental support for dynamics occurring on this timescale (40). Thus, for covalent reactions of small molecules, estimates of the intrinsic barrier from rate-equilibrium relationships can generate accurate order-of-magnitude predictions of the pre-exponential factor and thus the timescale of the dynamics underlying the reaction.

It is necessary to have a model of the reaction surface to estimate the intrinsic barrier from $\delta\phi/\delta\Delta G$. In the Appendix we derive an equation that relates $\delta\phi/\delta\Delta G$ to the intrinsic energy barrier, γ, for a reaction surface having two orthogonal parabolic reaction coordinates, with one reaction coordinate representing the motions of the residue probed by the REFER analysis and the other reaction coordinate representing the motions of the residue of the background mutation. If motions along the two reaction coordinates have similar mechanical properties (i.e., the curvature of the free energy surface is similar along both reaction coordinates), $\partial\phi/\partial\Delta G^B = 1/4\gamma$. From this equation and the observed overall $\delta\phi/\delta\Delta G$ value of $-0.075/k_BT$ for di-liganded gating, $\gamma = 3.3 \pm 0.9\ k_BT$. From Eq. 1 we calculate $A = 5 \times 10^4\ s^{-1}$, which is of the same order of magnitude as the opening rate constant for wild-type AChR activated by ACh (41).

These estimates are different from those obtained by Chakrapani and Auerbach. However, for a protein conformational change, the shape of the potentials is not required to be parabolic (42,43). Therefore, one possible reason for this discrepancy is that the quantitative treatment described in the Appendix is not applicable to the AChR gating reaction, which leads to an underestimation of γ. Another possibility is that a limit in the channel-closing rate constant influences the measured ϕ for the εP121L and εP121L+αT422A. A limit for the closing rate constant (~12,000 s^{-1}) would produce artificially high ϕ in constructs that reached the limit, since their opening rates could still decrease, but their closing rates could not increase. If we exclude the εP121L and εP121L+αT422A constructs and use the $\delta\phi/\delta\Delta G$ value of $-0.048/k_BT$ derived from comparing the wild-type background to the αT422A background, we estimate $\gamma = 5.2\ k_BT$ and $A = 3.7 \times 10^5\ s^{-1}$, which are closer to the values estimated by Chakrapani and Auerbach using the burst duration asymptote.

The results of this study are consistent with a view of the AChR gating reaction in which shallow potential energy surfaces give rise to a relatively small intrinsic barrier to gating. A shallow potential energy surface allows the transition state to be plastic, responding to energetic perturbations by altering its structure. It thus appears that during gating, the channel structure is somewhat fluid and able to sample multiple conformations.

APPENDIX

Here we present a simple model that uses two reaction coordinates to account for the effects of energetic perturbations on AChR gating kinetics. We assume that mutations are energetically independent of each other, and that the motions of each individual residue constitute a reaction coordinate. We consider two residues, *A* (the residue probed in the REFER analysis) and *B* (the background mutation). We will call the closed state C^AC^B and the open state O^AO^B (Fig. 6) to indicate that in these states, residues *A* and *B* are both in their closed/open conformation. We can also define states O^AC^B and C^AO^B, where one residue is in its open conformation while the other is in its closed conformation. It is important to note that these intermediate states are not directly observable: with a dead-time of ~25 μs, AChR gating appears as a two-state process with no observable intermediates. These intermediate states can be thought of as local maxima on the free energy surface, or perhaps local minima that are sufficiently high in energy that the reaction does not proceed through them.

To describe the free energy surface defined by our two reaction coordinates, we define a number of free energy differences (Fig. 6). ΔG is the free energy difference between the open and closed states. It can be determined experimentally from the gating equilibrium constant ($\Delta G = -kT \ln\Theta$). $\Delta G'$ is the free energy difference between O^AC^B and C^AO^B (which cannot be determined directly). The free energy differences associated with either residue *A* or residue *B* changing conformation, but not both, are defined as ΔG^{AC}, ΔG^{BO}, ΔG^{BC}, and ΔG^{AO} as in Fig. 6. These free energy differences correspond to the contribution of each individual residue to the gating free energy; they, too, cannot be determined directly.

With the assumption that the sites are energetically independent so that the free energies associated with mutations are additive, we obtain

$$\Delta G = \Delta G^{AC} + \Delta G^{OB} = \Delta G^{BC} + \Delta G^{AO}, \quad (2a)$$

$$\Delta G' = \Delta G^{AO} - \Delta G^{OB} = \Delta G^{AC} - \Delta G^{CB}. \quad (2b)$$

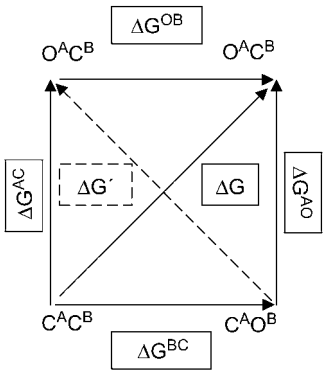

FIGURE 6 Two-dimensional free energy versus reaction coordinate diagram. The conformations of two residues, *A* and *B*, as the channel goes from closed (*C*) to open (*O*), are considered as reaction coordinates. The lower left-hand corner corresponds to the closed state of AChR and the upper right-hand corner corresponds to the open state. The gating reaction is represented by the solid arrow: its free energy of reaction is ΔG (*solid box*, the difference in free energy between the states at the *top right* and the *bottom left*). The other corners represent states where one residue is in the open conformation and the other is in the closed conformation: these are not observed experimentally, and are likely to be local maxima on the energy surface or high energy minima. The free energy difference between these two states is $\Delta G'$ (*dashed arrow* and *box*, the difference in free energy between the states at the *top left* and *bottom right*). The other free energy differences (ΔG^{AC}, ΔG^{OB}, ΔG^{AO}, and ΔG^{CB}) are the differences between adjacent corners in the diagram; i.e., the free energy differences associated with a single residue adopting its open or closed conformation.

The assumption of energetic independence also implies that $\Delta G^{AC} = \Delta G^{AO}$ and $\Delta G^{CB} = \Delta G^{OB}$. Defining $\Delta G^{A} = \Delta G^{AC} = \Delta G^{AO}$ and $\Delta G^{B} = \Delta G^{CB} = \Delta G^{OB}$, we obtain

$$\Delta G = \Delta G^{A} + \Delta G^{B}, \tag{3a}$$

$$\Delta G' = \Delta G^{A} - \Delta G^{B}. \tag{3b}$$

For two reaction coordinates, the equation relating equilibrium free energies to the activation energy is (11),

$$\Delta G^{\ddagger} = \gamma + 1/2(\Delta G) + \frac{(\Delta G)^2}{16\gamma} - \frac{(\Delta G')^2}{16\mu}, \tag{4}$$

where $\Delta G^{\ddagger}$ is the activation energy and γ and μ are parameters representing the curvature of the free energy surface. The γ-parameter is the intrinsic barrier for gating.

Substituting Eqs. 3a and 3b into Eq. 4, we obtain

$$\Delta G^{\ddagger} = \gamma + 1/2(\Delta G) + \frac{(\Delta G^{A} + \Delta G^{B})^2}{16\gamma} - \frac{(\Delta G^{A} - \Delta G^{B})^2}{16\mu}. \tag{5}$$

The ϕ-value is defined as $\phi = \partial\Delta G^{\ddagger}/\partial\Delta G^{A}$. Energetic independence of sites implies that $\partial\Delta G^{B}/\partial\Delta G^{A} = \partial\Delta G^{A}/\partial\Delta G^{B} = 0$, so

$$\phi = 1/2 + \frac{(\Delta G^{A} + \Delta G^{B})}{8\gamma} - \frac{(\Delta G^{A} - \Delta G^{B})}{8\mu}. \tag{6}$$

In the absence of a background mutation, the curvature of the REFER plot, $\partial\phi/\partial\Delta G^{A}$, is thus given by

$$\partial\phi/\partial\Delta G^{A} = \frac{1}{8\gamma} - \frac{1}{8\mu}. \tag{7}$$

Experimentally, these curvatures are not significantly different from zero. It is likely that curvatures of magnitude $>0.01\ kT^{-1}$ (either positive or negative) would be observable (a difference of 0.1 in ϕ, over three orders of magnitude in the equilibrium constant). For values of $\gamma < 10$ kT, this means that γ and μ differ by a factor of 5 or less. Here, we will make the simplifying assumption that $\mu = \gamma$. It is consistent with the REFER data and allows us to obtain a rough estimate of γ. Physically, this assumption is equivalent to assuming that the mechanical stiffness associated with gating is equal for the two residues.

The dependence of ϕ on energetic perturbations at a background residue is $\partial\phi/\partial\Delta G^{B}$. This is the slope of the plot in Fig. 5. Differentiating Eq. 6 with respect to ΔG^{B}, we obtain

$$\partial\phi/\partial\Delta G^{B} = \frac{1}{8\gamma} + \frac{1}{8\mu}. \tag{8}$$

Using the assumption that $\mu = \gamma$, this gives $\partial\phi/\partial\Delta G^{B} = (1/4\gamma)$, the expression used in the main text.

Of course, if $\mu \neq \gamma$, this expression does not hold. In the limit where $\mu \gg \gamma$, $\partial\phi/\partial\Delta G^{B} \cong (1/8\gamma)$, the same as in the one-dimensional analysis. In the limit where $\mu \ll \gamma$, $\partial\phi/\partial\Delta G^{B} \cong (1/8\mu)$. In that case, the effects of the background mutation on ϕ would be due to a change in transition state structure/energetics along the reaction coordinate representing the motions of residue *B*, the background residue.

We thank members of the Auerbach and Sachs laboratories for helpful discussions.

This work was supported by the National Institutes of Health (No. NS-23513). S.L. was supported by a National Institutes of Health postdoctoral fellowship (NRSA No. F32 GM63460-02).

REFERENCES

1. Miyazawa, A., Y. Fujiyoshi, and N. Unwin. 2003. Structure and gating mechanism of the acetylcholine receptor pore. *Nature*. 423:949–955.
2. Perozo, E., D. M. Cortes, and L. G. Cuello. 1999. Structural rearrangements underlying K^+-channel activation gating. *Science*. 285: 73–78.
3. Liu, Y. S., P. Sompornpisut, and E. Perozo. 2001. Structure of the KcsA channel intracellular gate in the open state. *Nat. Struct. Biol.* 8: 883–887.
4. Jiang, Y. X., A. Lee, J. Y. Chen, V. Ruta, M. Cadene, B. T. Chait, and R. MacKinnon. 2003. X-ray structure of a voltage-dependent K^+ channel. *Nature*. 423:33–41.
5. Jiang, Y. X., A. Lee, J. Y. Chen, M. Cadene, B. T. Chait, and R. MacKinnon. 2002. The open pore conformation of potassium channels. *Nature*. 417:523–526.
6. Grosman, C., M. Zhou, and A. Auerbach. 2000. Mapping the conformational wave of acetylcholine receptor channel gating. *Nature*. 403:773–776.
7. Chakrapani, S., T. D. Bailey, and A. Auerbach. 2004. Gating dynamics of the acetylcholine receptor extracellular domain. *J. Gen. Physiol.* 123:341–356.
8. Jencks, W. P. 1985. A primer for the Bema Hapothle. An empirical approach to the characterization of changing transition state structures. *Chem. Rev.* 85:511–527.
9. Jencks, D. A., and W. P. Jencks. 1977. On the characterization of transition states by structure-reactivity coefficients. *J. Am. Chem. Soc.* 99:7948–7960.

10. Jencks, W. P. 1972. General acid-base catalysis of complex reactions in water. *Chem. Rev.* 72:705–718.

11. Grunwald, E. 1985. Structure-energy relations, reaction mechanism, and disparity of progress of concerted reaction events. *J. Am. Chem. Soc.* 107:125–133.

12. Fersht, A. R. 1995. Characterizing transition states in protein folding—an essential step in the puzzle. *Curr. Opin. Struct. Biol.* 5: 79–84.

13. Onuchic, J. N., N. D. Socci, Z. Luthey-Schulten, and P. G. Wolynes. 1996. Protein folding funnels: the nature of the transition state ensemble. *Fold. Des.* 1:441–450.

14. Fersht, A. R., R. J. Leatherbarrow, and T. N. Wells. 1987. Structure-activity relationships in engineered proteins: analysis of use of binding energy by linear free energy relationships. *Biochemistry.* 26:6030–6038.

15. Toney, M. D., and J. F. Kirsch. 1989. Direct Brønsted analysis of the restoration of activity to a mutant enzyme by exogenous amines. *Science.* 243:1485–1488.

16. Eaton, W. A., E. R. Henry, and J. Hofrichter. 1991. Application of linear free energy relations to protein conformational changes: the quaternary structural change of hemoglobin. *Proc. Natl. Acad. Sci. USA.* 88:4472–4475.

17. Yifrach, O., and A. Horovitz. 1998. Mapping the transition state of the allosteric pathway of GroEL by protein engineering. *J. Am. Chem. Soc.* 120:13262–13263.

18. Mitra, A., T. D. Bailey, and A. L. Auerbach. 2004. Structural dynamics of the M4 transmembrane segment during acetylcholine receptor gating. *Structure.* 12:1909–1918.

19. Chakrapani, S., T. D. Bailey, and A. Auerbach. 2003. The role of loop 5 in acetylcholine receptor channel gating. *J. Gen. Physiol.* 122:521–539.

20. Oliveberg, M., Y. J. Tan, M. Silow, and A. R. Fersht. 1998. The changing nature of the protein folding transition state: implications for the shape of the free-energy profile for folding. *J. Mol. Biol.* 277:933–943.

21. Grosman, C. 2003. Free-energy landscapes of ion-channel gating are malleable: changes in the number of bound ligands are accompanied by changes in the location of the transition state in acetylcholine-receptor channels. *Biochemistry.* 42:14977–14987.

22. Chakrapani, S., and A. Auerbach. 2005. A speed limit for conformational change of an allosteric membrane protein. *Proc. Natl. Acad. Sci. USA.* 102:87–92.

23. Qin, F. 2004. Restoration of single-channel currents using the segmental *k*-means method based on hidden Markov modeling. *Biophys. J.* 86:1488–1501.

24. Qin, F., A. Auerbach, and F. Sachs. 1997. Maximum likelihood estimation of aggregated Markov processes. *Proc. Roy. Soc. Lond. B Biol.* 264:375–383.

25. Qin, F., A. Auerbach, and F. Sachs. 2000. A direct optimization approach to hidden Markov modeling for single channel kinetics. *Biophys. J.* 79:1915–1927.

26. Grosman, C., and A. Auerbach. 2001. The dissociation of acetylcholine from open nicotinic receptor channels. *Proc. Natl. Acad. Sci. USA.* 98:14102–14107.

27. Zhou, M., A. G. Engel, and A. Auerbach. 1999. Serum choline activates mutant acetylcholine receptors that cause slow channel congenital myasthenic syndromes. *Proc. Natl. Acad. Sci. USA.* 96: 10466–10471.

28. Grosman, C., and A. Auerbach. 2000. Asymmetric and independent contribution of the second transmembrane segment 12′ residues to diliganded gating of acetylcholine receptor channels: a single-channel study with choline as the agonist. *J. Gen. Physiol.* 115:637–651.

29. Bouzat, C., F. Barrantes, and S. Sine. 2000. Nicotinic receptor fourth transmembrane domain—hydrogen bonding by conserved threonine contributes to channel gating kinetics. *J. Gen. Physiol.* 115: 663–671.

30. Ohno, K., H. L. Wang, M. Milone, N. Bren, J. M. Brengman, S. Nakano, P. Quiram, J. N. Pruitt, S. M. Sine, and A. G. Engel. 1996. Congenital myasthenic syndrome caused by decreased agonist binding affinity due to a mutation in the acetylcholine receptor ε-subunit. *Neuron.* 17:157–170.

31. Marcus, R. A. 1968. Theoretical relations among rate constants, barriers, and Brønsted slopes of chemical reactions. *J. Phys. Chem.* 72:891–899.

32. Karlin, A., and M. H. Akabas. 1995. Toward a structural basis for the function of nicotinic acetylcholine receptors and their cousins. *Neuron.* 15:1231–1244.

33. Cymes, G. D., C. Grosman, and A. Auerbach. 2002. Structure of the transition state of gating in the acetylcholine receptor channel pore: a ϕ-value analysis. *Biochemistry.* 41:5548–5555.

34. Unwin, N. 2005. Refined structure of the nicotinic acetylcholine receptor at 4 Ångström resolution. *J. Mol. Biol.* 346:967–989.

35. Jonsson, T., C. D. Waldburger, and R. T. Sauer. 1996. Nonlinear free energy relationships in arc repressor unfolding imply the existence of unstable, native-like folding intermediates. *Biochemistry.* 35:4795–4802.

36. Oliveberg, M. 1998. Alternative explanations for ''multistate'' kinetics in protein folding: transient aggregation and changing transition-state ensembles. *Acc. Chem. Res.* 31:765–772.

37. Miyashita, O., J. N. Onuchic, and P. G. Wolynes. 2003. Nonlinear elasticity, proteinquakes, and the energy landscapes of functional transitions in proteins. *Proc. Natl. Acad. Sci. USA.* 100:12570–12575.

38. Miyashita, O., P. G. Wolynes, and J. N. Onuchic. 2005. Simple energy landscape model for the kinetics of functional transitions in proteins. *J. Phys. Chem. B.* 109:1959–1969.

39. Portman, J. J., S. Takada, and P. G. Wolynes. 2001. Microscopic theory of protein folding rates. II. Local reaction coordinates and chain dynamics. *J. Chem. Phys.* 114:5082–5096.

40. Zewail, A. H. 2000. Femtochemistry: atomic-scale dynamics of the chemical bond using ultrafast lasers (Nobel lecture). *Angew. Chem. Int. Ed. Engl.* 39:2587–2631.

41. Maconochie, D. J., and J. H. Steinbach. 1998. The channel opening rate of adult- and fetal-type mouse muscle nicotinic receptors activated by acetylcholine. *J. Physiol. (Lond.).* 506:53–72.

42. Auerbach, A. 2005. Gating of acetylcholine receptor channels: Brownian motion across a broad transition state. *Proc. Natl. Acad. Sci. USA.* 102:1408–1412.

43. Zhou, Y., J. E. Pearson, and A. Auerbach. 2005. Phi-value analysis of a linear, sequential reaction mechanism: theory and application to ion channel gating. *Biophys. J.* In press.